analytical chemistry

ARTICLE

pubs.acs.org/ac

Shift Reagents for Multidimensional Ion Mobility Spectrometry-Mass Spectrometry Analysis of Complex Peptide Mixtures: Evaluation of 18-Crown-6 Ether Complexes

Brian C. Bohrer and David E. Clemmer*

Department of Chemistry, Indiana University, Bloomington, Indiana 47405, United States

ABSTRACT:

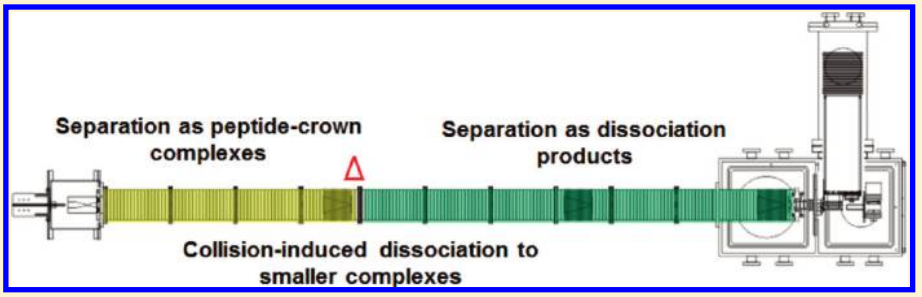

18-Crown-6 ether (18C6) is evaluated as a shift reagent for multidimensional ion mobility spectrometry-mass spectrometry (IMS-IMS-MS) analyses of tryptic protein digests. In this approach, 18C6 is spiked into the solution-phase mixture and noncovalent peptide−crown ion complexes are formed by electrospraying the mixture into the gas phase. After an initial mobility separation in the first IMS drift region, complexes of similar mobility are selected and dissociated via collisional activation prior to entering the second drift region. These dissociation products (including smaller complexes, naked peptide ions, charge transfer products, and fragment ions) differ in mobility from their precursor ion complexes and (in favorable cases) from one another, allowing the mixture to resolve further in the second IMS region. We estimate an IMS-IMS peak capacity of ∼2400 when shift reagents are employed. The approach is illustrated by examining a tryptic digest of cytochrome *c* and by identifying a peptide out of a complex mixture obtained by digestion of human plasma proteins. Disadvantages arising from increased complexity of data sets as well as other advantages of this approach are considered.

Ion mobility spectrometry (IMS) coupled to mass spectrometry (MS) is becoming widely used in the analysis of complex mixtures, such as those encountered in the emerging areas of proteomics, metabolomics, and glycomics.[1−15] One factor that limits this combination is that IMS separates ions based on differences in their sizes (or average collision cross section) while MS separates based on differences in ion masses, and these properties are intrinsically correlated. In several recent reports, we have described the development of multidimensional IMS-MS (IMS-IMS-MS and IMS-IMS-IMS-MS)[16,17] analyses of peptides and proteins.[17−21] With these techniques, we aim to alter the intrinsic correlation of ion size and mass by changing the ions' shapes. This can improve the detection of low-intensity signals and increase the analytical peak capacity (important for many-component mixtures).[22] Merenbloom et al. demonstrated a peak capacity for an IMS-IMS separation of peptides (prior to MS) in excess of 1000.[22] While this is substantial, the approach is fundamentally restricted by the extent to which structures change upon collisional activation. In favorable cases, cross sections can be altered by as much as ±11% upon activation.[22] However, for many ions, collisional activation results in little change in the overall ion shape (often only a few percent change in cross section is observed).[22] In cases where no change in mobility can be induced, the multidimensional separation offers no advantage relative to a single IMS separation.

In this paper we use an IMS shift reagent[23,24] to increase the differences in mobility between analyte ions studied before and after activation. Shift reagents are molecules that form noncovalent adducts with analyte species (either in solution or during the ionization process) to produce ion complexes.[23,24] We have previously examined the use of 18-crown-6 ether (18C6) as a shift reagent and illustrated a method that utilizes a single IMS dimension to resolve three isobaric tripeptides that form peptide−crown complexes.[23] In an IMS-IMS analysis using shift reagents, analytes initially separate as a mixture of adduct ions and are subsequently collisionally activated such that smaller complexes (or naked ions) can be separated in a second IMS region. Below, we investigate the advantages of shift reagents with peptides generated by digestion of proteins with trypsin.[25] Proteolytic digestion is a common method of generating peptide mixtures for "bottom-up" proteomics studies.[25] Trypsin cleaves proteins at basic arginine and lysine residues and thus couples

Received: April 7, 2011
Accepted: May 24, 2011
Published: May 24, 2011

favorably with the affinity of crown ethers for protonated amine moieties.[26−28] We assess the utility of combining shift reagents with IMS-IMS by examining peptides obtained upon tryptic digestion of cytochrome *c*. Upon assessing the overall approach, we illustrate an application of this method by the identification of a peptide from an extremely complex mixture, human plasma.

The present work is closely related to a number of fundamental studies involving the binding of crown ethers to amines.[26−28] These systems have been useful models in the study of molecular recognition,[27−29] gas-phase hydrogen/deuterium exchange,[26] and the mobile proton model in the context of collision-induced dissociation (CID) of peptide ions.[26] As described by others,[28] the presence of 18C6 in the electrospray solution is found to alter the ionization efficiency as well as the charge state distributions of many peptide ions. A recent report suggests that measurements of these complexes are sensitive to molecular motion within supramolecular complexes.[30] We also discuss some features pertaining to the structures of peptide−crown complexes.

EXPERIMENTAL SECTION

Instrumentation. General discussions of IMS experiments and theory as well as IMS-MS combinations have been reported elsewhere.[1,16,31−35] Experiments reported here were conducted on two similar home-built IMS-IMS-MS instruments differing mainly in the total length of the drift tube. Early studies were conducted on a drift tube roughly 2 m in length; later experiments were conducted on a drift tube ∼3 m in length. Only a short description of these instruments is provided here; a detailed report has been published previously.[16] Briefly, electrosprayed ions are accumulated in a source ion funnel and are released in 150 μs-wide pulses into the drift tube where they diffuse through a buffer gas (∼3.0 Torr He at 300 K) under the influence of a weak uniform electric field (9 V cm^{-1}). For IMS-IMS experiments, the total drift tube length is divided into two drift regions separated by an electrostatic gate used to transmit mobility-selected ions. The selection of these ions is defined by a variable delay that is triggered by the source pulse of the drift experiment. Selected ions are then heated through high-field collisions in an ion activation region to produce a new distribution of ions prior to entering the second drift region. The extent of activation can be tuned by changing the voltage drop across the lenses (spaced ∼0.3 cm apart) comprising the activation region. A difference of 5 V is used for passive transmission of ions, whereas 200 V difference or greater leads to substantial CID of peptide ions. In these studies, activation voltages of 125 and 165 V were examined for dissociation of noncovalent complexes. Upon exiting the drift tube, the ions enter the source of an orthogonal reflectron time-of-flight (TOF) mass spectrometer. For the types of ions investigated here, we estimate this mass analyzer exhibits a resolution of ∼2500 with a mass accuracy of ∼0.4 Da. Because the time scale of TOF analysis is 3 orders of magnitude smaller than that of the IMS analysis (tens of microseconds compared to tens of milliseconds), roughly one thousand mass spectra are collected over the course of a single drift separation. Nested measurements of drift times (t_D) and m/z are collected to construct the IMS-MS data as described previously.[36,37] We report t_D and m/z values using the $t_D(m/z)$ nomenclature convention described elsewhere.[36]

Sample Preparation and Electrospray Conditions. Cytochrome *c* (horse heart, 90% purity from Sigma, St. Louis, MO) was digested with trypsin using standard procedures described previously.[22] The lyophilized product was prepared for electrospray ionization (ESI) in solution (49:49:2 water−acetonitrile−acetic acid) at a concentration of 0.25 mg mL^{-1}. Plasma samples were prepared with abundant proteins depleted as previously reported.[18] The plasma peptides were dissolved in 49:49:2 water−acetonitrile−acetic acid and brought to an estimated total peptide concentration of ∼0.3 mg/mL. Noncovalent complexes were formed by addition of 50 mol equiv of 18-crown-6 ether (99% purity, Aldrich, St. Louis, MO) to an aliquot of the digest solutions. A syringe pump (*kd* Scientific, Holliston, MA) was used to deliver sample at a flow rate of 0.25 μL min^{-1} through a pulled capillary tip (75 μm i.d. × 360 μm o.d.) biased 2.2 kV above the drift voltage.

Cross Section Measurements. Drift times measured for peptides and peptide−crown complexes can be converted into collision cross sections using the following equation[38]

$$\Omega = \frac{(18\pi)^{1/2}}{16}\frac{ze}{(k_B T)^{1/2}}\left[\frac{1}{m_I}+\frac{1}{m_B}\right]^{1/2}\frac{t_D E}{L}\frac{760}{P}\frac{T}{273.2}\frac{1}{N} \quad (1)$$

where ze is the charge of the ion, k_B is Boltzmann's constant, and T refers to the temperature of the buffer gas. Values m_I and m_B correspond to the masses of the ion and buffer gas (in this case, He atoms), respectively. The measured drift times are represented by t_D, and parameters L, P, and N correspond to the length of the drift separation, the buffer gas pressure, and the buffer gas number density, respectively.

Database Search for Peptide Identifications. Peptides from human plasma were assigned using database searches. Fragment peak lists were compiled into text files and searched against the Swis-Prot human database using a MASCOT software suite.[39] To allow for the presence of the remaining 18C6 adducts, the precursor mass used in the search was adjusted to account for neutral losses of this species. As part of the MASCOT search, a threshold score is generated to indicate the statistical relevance of the matched results.

RESULTS AND DISCUSSION

IMS-MS Data Sets for Peptides and Peptide−Crown Complexes. Figure 1 shows the nested $t_D(m/z)$ distributions for the tryptic peptides of cytochrome *c* and the corresponding peptide−18C6 mixture. Experimentally determined m/z values and cross sections (converted from experimental drift times using eq 1) are in agreement with those reported previously.[40] A theoretical peak list for peptide−crown complexes was constructed using the monoisotopic mass of 18C6 (264.16 Da), and a summary of assignments is provided in Tables 1 and 2. The nomenclature used for assignments is as follows. The first number in the label (Figure 1 and Tables 1 and 2) corresponds to the charge state of the ion. A letter is assigned to the peptide sequence in alphabetical order with increasing peptide mass. For peptide−crown complexes, a second number is added to denote the number of adducts on the ion. As described previously,[41] ions of the same charge state fall into families and are shown by the white diagonal lines labeled $[M + H]^+$, $[M + 2H]^{2+}$, $[M + 3H]^{3+}$, and $[M + 4H]^{4+}$. Intense peaks observed at low m/z have been assigned as $[18C6 + H]^+$, $[18C6 + H_2O + H]^+$, $[18C6 + Na]^+$, and $[18C6 + K]^+$ and appear at 10.9(265.2), 10.9(283.2), 10.5(287.1), and 11.0(303.3), respectively.

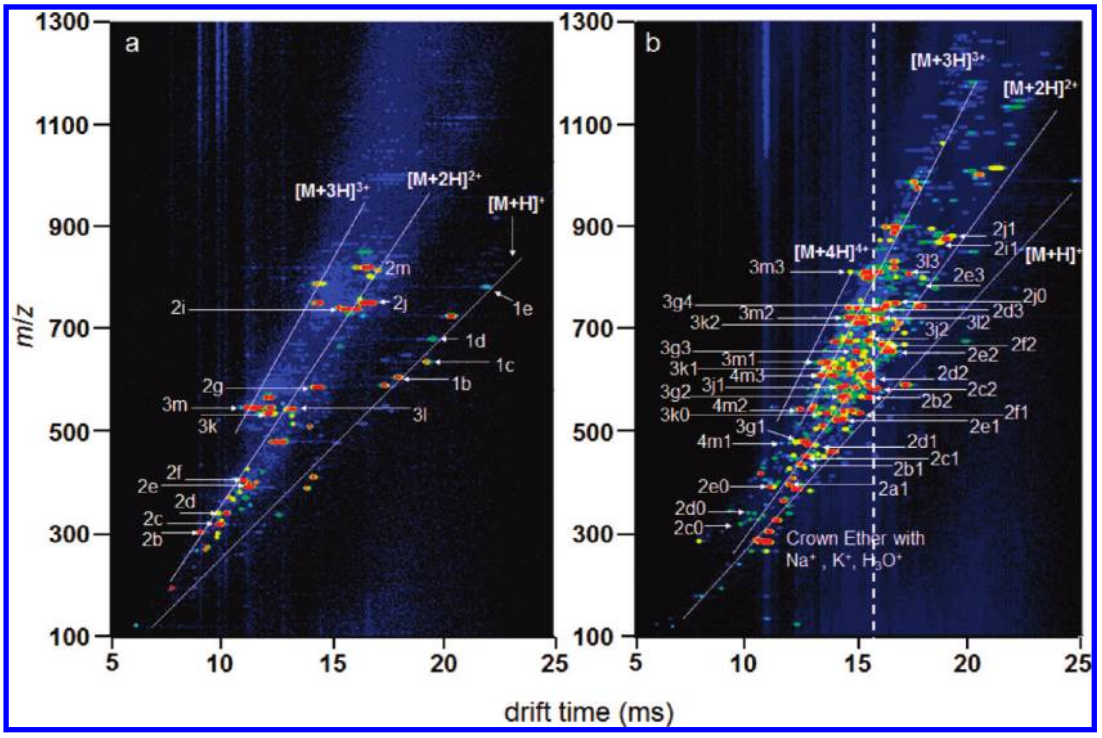

Figure 1. Two nested $t_D(m/z)$ plots for a tryptic digest of equine cytochrome *c* sprayed alone (a) and with 18C6 (b). Diagonal lines depicting the general location of the observed charge states are labeled on each graph. The vertical line on part b shows the selections made in the experiments shown in Figure 2. Assignments for peak labels can be found in Tables 1 and 2 for parts a and b of Figure 1, respectively. The first number corresponds to the charge state, the letter was alphabetically assigned to the observed peptides in order of increasing neutral mass, and the second number distinguishes the number of crown ether adducts associated with the peptide.

Table 1. Peptides Observed in IMS-MS Analysis of Cytochrome *c* Digest

peptide sequence	sequence label[a]	neutral mass[b]	$[M + H]^{+c}$	$[M + 2H]^{2+c}$	$[M + 3H]^{3+c}$
GGKHK	a	525.30			
GITWK	b	603.34	1b	2b	
IFVQK	c	633.38	1c	2c	
YIPGTK	d	677.37	1d	2d	
MIFAGIK	e	778.44	1e	2e	
KYIPGTK	f	805.47		2f	
TGPNLHGLFGR	g	1167.61		2g	
YIPGTKMIFAGIK	h	1437.80			
TGQAPGFTYTDANK	i	1469.68		2i	
EETLMEYLENPK	j	1494.69		2j	
KTGQAPGFTYTDANK	k	1597.77		2k	3k
EETLMEYLENPKK	l	1622.79		2l	
IFVQKCAQCHTVEK	m	1632.81		2m	3m

[a] Each peptide observed was assigned a letter alphabetically with increasing neutral mass for ease of use in discussion and labeled spectra. [b] Monoisotopic neutral masses calculated using in silico digestion. [c] To specify a peak, the sequence label is preceded by a number corresponding to the charge state at which it was observed.

Inspection of these data in Figure 1 shows that the spectrum for the peptide−crown mixture contains many more peaks compared to the data for the peptide sample. Most of the additional peaks are associated with variations in the binding stoichiometry between 18C6 and the peptides. For example, consider the peak 2g in Figure 1 at $t_D(m/z)$ = 14.3(584.8). Upon addition of 18C6, the same peptide is represented by peaks 3g1, 3g2, 3g3, and 3g4, present at 12.6(478.3), 14.4(566.3), 15.0(654.4), and 16.2(742.4), respectively. This is a general feature of the system and results in each peak in Figure 1a splitting into multiple peaks in Figure 1b. Some additional peaks are associated with peptide sequences that are detected exclusively in the sample with 18C6. These sequences (GGKHK and YIPGTKMIFAGIK) correspond to missed cleavages and are presumably present at a lower abundance in solution. It seems likely that the increased electrospray ionization efficiency afforded by complexation with 18C6 (as observed previously by us

dx.doi.org/10.1021/ac200892r |*Anal. Chem.* 2011, 83, 5377–5385

Table 2. Peptides Observed in IMS-IMS-MS Analysis of Cytochrome *c* Digest Using Shift Reagents

peptide sequence	neutral mass	charge states	values of *n*
GGKHK	525.30	$[M + n(18C6) + 2H]^{2+}$	1−3 (2a1−2a3)[a]
GITWK	603.34	$[M + n(18C6) + 2H]^{2+}$	0−3 (2b0−2b3)
IFVQK	633.38	$[M + n(18C6) + 2H]^{2+}$	0−3 (2c0−2c3)
YIPGTK	677.37	$[M + n(18C6) + 2H)^{2+}$	0−3 (2d0−2d3)
MIFAGIK	778.44	$[M + n(18C6) + 2H]^{2+}$	1−3 (2e1−2e3)
KYIPGTK	805.47	$[M + n(18C6) + 2H]^{2+}$	1−3 (2f1−2f3)
TGPNLHGLFGR	1167.61	$[M + n(18C6) + 3H]^{3+}$	1−4 (3g1−3g4)
YIPGTKMIFAGIK	1437.80	$[M + n(18C6) + 3H]^{3+}$	1 (3h1)
TGQAPGFTYTDANK	1469.68	$[M + n(18C6) + 2H]^{2+}$	1 (2i1)
EETLMEYLENPK	1494.69	$[M + n(18C6) + 2H]^{2+}$	0−1 (2j0−2j1)
		$[M + n(18C6) + 3H]^{3+}$	1−2 (3j1−3j2)
KTGQAPGFTYTDANK	1597.77	$[M + n(18C6) + 3H]^{3+}$	0−4 (3k0−3k4)
EETLMEYLENPKK	1622.79	$[M + n(18C6) + 3H]^{3+}$	1−4 (3l1−3l4)
IFVQKCAQCHTVEK	1632.81	$[M + n(18C6) + 2H]^{2+}$	1−2 (2m1−2m2)
		$[M + n(18C6) + 3H]^{3+}$	1−4 (3m1−3m4)
		$[M + n(18C6) + 4H]^{4+}$	1−2 (4m1−4m2)

[a] Peak labels follow the same notation as Table 1 with one addition; the number at the end of the label denotes the number of 18C6 adducts complexed to the ion.

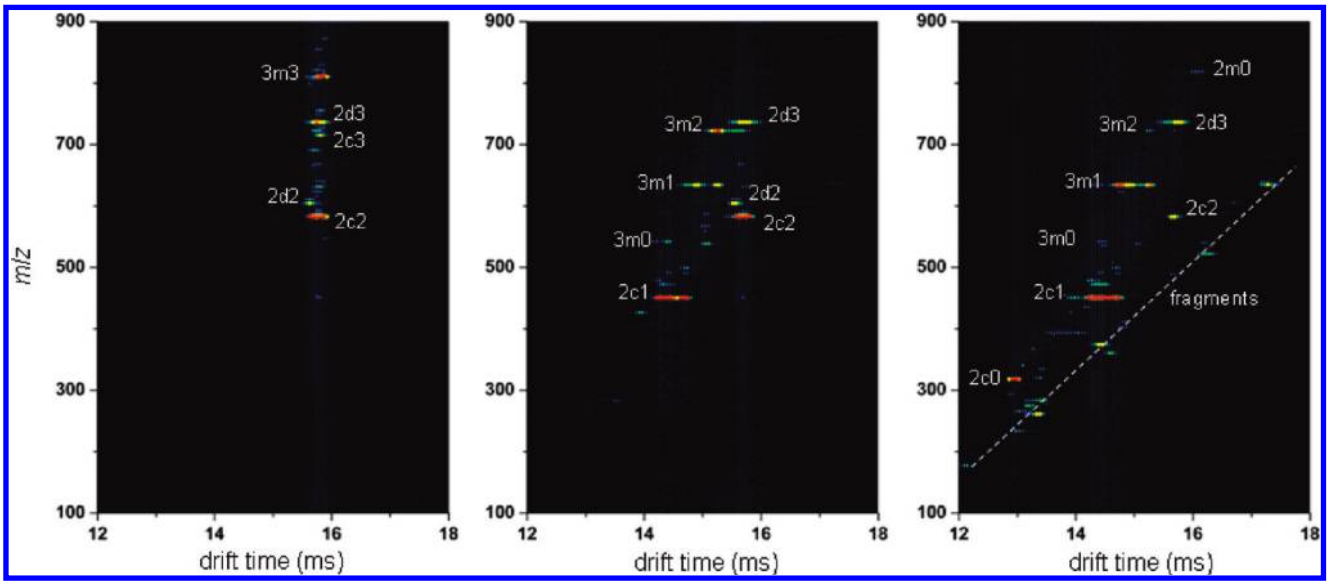

Figure 2. A selected packet of ions with total drift times in the range of 15.52−15.73 ms is transmitted with no activation (left panel), with activation at 125 (middle panel) and 165 V (right panel).

and others)[28] is responsible for the detection of these peptides. This feature of the complexation analysis is potentially useful in proteomic analyses, where detection of multiple peptides is often required for identification of a protein.[42]

Another feature of the complexation analysis with 18C6 is observation of ions at higher charge states. While the peptides identified from the typical ESI solution produced ions with z = 1−3, peptide−crown complex ions are found with z = 2−4. The charge increase results from stabilization of the charged sites.[28] Additionally, higher charge states may be facilitated by dielectric shielding of the charged site upon binding 18C6. It is worth noting that peaks corresponding to complexes are similar in width to those without 18C6 adducts. It appears that peaks do not broaden upon complex formation.

IMS-IMS Analysis of Peptide−Crown Complexes. Figure 2 shows a blown up region of the nested data sets corresponding to a mobility selection that leads to a total drift time at the vertical dashed line in Figure 1 (15.52−15.72 ms total drift time). Additionally, plots of data recorded at two collisional activation voltages (125 and 165 V) are shown. The spectrum for the selection (left panel) is dominated by peaks 3m3, 2d3, 2c3, 2d2, and 2c2. Collisional activation of the selected ions at 125 V, shown in Figure 2 (middle), is generally sufficient to remove at least one 18C6 adduct from the complexes, generating the peaks 3m2 and 2c1 at 15.2(721.4) and 14.4(449.8) as the major products. At higher voltages (165 V, Figure 2, right) a greater extent of dissociation is observed and some portion of the bare peptides are recovered. Evidence for this is found from peak 2c0

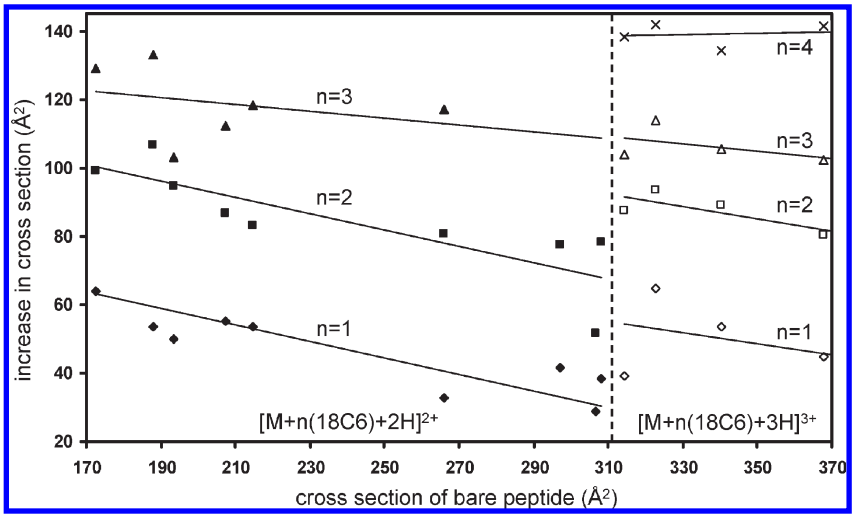

Figure 3. Effect of peptide or peptide−crown complex on shift magnitude afforded by multiple additions of 18C6. Cross section of the bare peptide is shown on the *x*-axis, and the increase in cross section upon complexation is shown on the *y*-axis. Data points that fall on a vertical line correspond to the same peptide ion from the cytochrome *c* digest. Single, double, triple, and quadruple additions of 18C6 are shown by diamonds, squares, triangles, and exes, respectively. Solid data points denote doubly charged ions, and open data points denote triply charged ions.

that is resolved in drift time at 12.9(317.7). This activation was also sufficient to produce some peptide fragment ions, shown by the labeled diagonal line. Evidence for charge reduction is also found. In this case, the small 2m0 peak corresponding to $[IFVQKCAQCHTVEK + 2H]^{2+}$ ion is likely produced from peaks 3m0 or 3m1 corresponding to $[IFVQKCAQCHTVEK + 3H]^{3+}$ and $[IFVQKCAQCHTVEK + 18C6 + 3H]^{3+}$, respectively. The $[18C6 + H]^{+}$ ion can be observed in some of the activated data sets (data not shown), suggesting that abstraction of the proton by the 18C6 adduct contributes to the charge transfer process.

Influence of Complexation on Cross Section. It is interesting to compare the cross sections of the peptide−crown complexes to those of the naked peptide ions. This can be done prior to complex formation and upon dissociation. Drift time distributions for some peptide ions are similar in appearance when compared to their complexed forms, with only a constant offset in total drift time. For example, the distribution for the peptide ion 3 m remains similar in its pattern for all peptide−crown stoichiometries observed. In these cases, it is tempting to assume that the backbone conformation of the peptide ion remains the same and the 18C6 ligands simply cap charged sites without structural distortion. In other examples, however, the drift time distributions change drastically (e.g., peptides that appear as singlets form multiplets upon complexation or vice versa). For example, although it appears predominantly as a single feature in the peptide-only sample, $[KTGQAPGFTYTDANK + 3H]^{3+}$ (peak 3k) appears as a doublet in its $[KTGQAPGFTYTDANK + 18C6 + 3H]^{3+}$ form (peak 3k1). In contrast, $[TGQAPGFTYTDANK + 2H]^{2+}$ (peak 2i) appears to adopt a narrower distribution of structures upon binding a single 18C6 adduct (peak 2i1). As such, there is very little that can be stated generally about the effect of 18C6 complexation on peptide structure; rather, the complexed form of a peptide ion appears to be sequence dependent in a way that is not straightforward to anticipate.

Comparison of Complexes with Different Numbers of Crowns. Some trends are apparent upon comparison of peptide−crown complexes of different sizes. The data in Figure 3 illustrates the effects of peptide size, degree of complexation, and charge state on the overall cross section of peptide−crown complexes. In this plot, a vertical line of points corresponds to the same peptide ion and the spacing between points represents the increasing cross section of a growing complex. Additionally, the effect of a given number of 18C6 adducts can be observed as the size of the peptide varies. As expected, larger peptides experience smaller increases in cross section upon complexation with 18C6 because the adduct comprises less of the total size of the complex for larger peptides. From Figure 3, we estimate the increase in size associated with incorporation of a crown on a peptide to be ∼20−40 Å^2.

It is interesting to compare cross sections of peptide ions formed directly by ESI and subsequently activated with those that arise upon dissociation of the peptide−crown complex. Overall, these cross sections are similar. This observation is consistent with studies of peptide conformer distributions that are produced upon collisional activation of isolated conformers.[43] It appears that, after dissociation, the activated ions continue to anneal, and the peptides form a relatively stable distribution of structures.

Assessing the Value of Complexation for Separation Capacity. Although addition of 18C6 clearly benefits IMS-IMS capabilities, the addition of this reagent also leads to a far more complex sample and more complicated data sets. Here we assess the enhancement gained compared to the cost of additional complexity. One means of quantifying this complexity is to compare the total number of peaks observed for a particular peptide sequence to the number observed for the peptide−crown complexes. We include different charge states and different numbers of 18C6 adducts, as each will appear as a unique peak. The ratio of these two numbers is the factor by which addition of 18C6 increases the complexity of the data set.

As an example, consider the MIFAGIK peptide. This peptide is observed as peaks 1e and 2e without addition of 18C6. In the presence of 18C6, three peaks from MIFAGIK were identified (2e1, 2e2, and 2e3). Additionally, 2e1 was present in a selection made in an IMS-IMS-MS experiment and produced the bare peptide (2e0). Thus, in total, four peaks related to the sequence

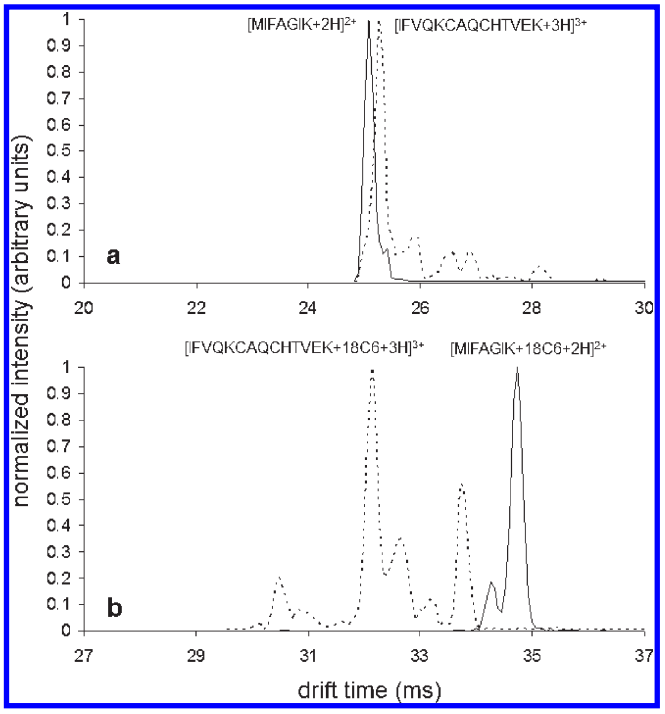

Figure 4. Total drift time distributions for two sequences of cytochrome *c* as analyzed by IMS-IMS (a). Same sequences analyzed by IMS-IMS with 18C6 shift reagent (b).

MIFAGIK are observed in the 18C6 spectrum. We conclude that the complexity for MIFAGIK is increased by a factor of 2. Extending this analysis to all peptide assignments allows us to estimate the average increase in complexity for all peptides in the digest. We find 17 assignments in IMS-MS analysis of peptides only, compared to 59 assignments in the peptide−crown mixture, an average complexity increase of a factor of ∼3.5.

These redundant peaks increase sample complexity but can provide valuable information. In cases where complexes appear at low abundance, or in a congested region of the spectrum, the increased complexity provides opportunities to detect (or select) ions. Finally, unique peaks from analyte ions that are only detected when electrosprayed with 18C6 add to the estimate of complexity above but provide valuable information that is otherwise absent.

An example of a favorable scenario is shown in Figure 4. IMS-IMS distributions for two peptide ions from cytochrome *c* digest, $[\text{MIFAGIK} + 2\text{H}]^{2+}$ and $[\text{IFVQKCAQCHTVEK} + 3\text{H}]^{3+}$, are shown. This plot corresponds to ions that were selected at 25.1 and 25.3 ms, respectively, and subsequently activated at 165 V. Although some of the $[\text{IFVQKCAQCHTVEK} + 3\text{H}]^{3+}$ ion population shifts to lower mobility, the majority remains close to the mobility at which it was selected. Thus, the IMS-IMS separation does not change the mobilities of these ions substantially, and significant overlap between the $[\text{IFQVKCAQCHTVEK} + 3\text{H}]^{3+}$ and $[\text{MIFAGIK} + 2\text{H}]^{2+}$ peaks remains. Figure 4 also shows an analogous experiment using 18C6 shift reagent. The precursors for this IMS-IMS separation were the $[\text{IFQVKCAQCHTVEK} + 2(18\text{C6}) + 3\text{H}]^{3+}$ and $[\text{MIFAGIK} + 2(18\text{C6}) + 2\text{H}]^{2+}$ ions, which were selected at 34 and 38 ms and activated to yield the $[\text{IFQVKCAQCHTVEK} + 18\text{C6} + 3\text{H}]^{3+}$ and $[\text{MIFAGIK} + 18\text{C6} + 2\text{H}]^{2+}$ ions. The shift in mobility observed upon 18C6 loss allows these species to be resolved. In addition to ensuring a shift occurs, the loss of 18C6 induces a shift that is larger than is typically associated with different peptide conformers.

Analysis of the peak widths, and the range over which peaks are observed, allows us to estimate the analytical peak capacity. Whereas the maximum observed shift in an IMS-IMS analysis of tryptic peptides was ±11%,[22] loss of a single 18C6 adduct shifts the peak in total drift time by ∼20−25%. Increased shifts in the second IMS region directly lead to higher two-dimensional peak capacity.[44] IMS-IMS analysis of $[\text{MIFAGIK} + n(18\text{C6}) + 2\text{H}]^{2+}$ ions (n = 1−3) gave rise to peaks with an average full-width-at-half-maximum (fwhm) value of 0.255 ms. These peaks are observed to extend over a range of 7.75 ms. Thus, we calculate a peak capacity of ∼30 (7.75 ms/0.255 ms). Peaks associated with the $[\text{IFVQKCAQCHTVEK} + n(18\text{C6}) + 3\text{H}]^{3+}$ ions (n = 1−4) had an average fwhm value of 0.233 ms and occupied a range of 6.88 ms, also resulting in a peak capacity of ∼30. The peak capacity of the initial drift separation is between 60 and 80 for tryptic peptide ions.[22] Therefore, the data reported here suggest a maximum total IMS-IMS peak capacity of between 1800 and 2400 when shift reagents are used. This is substantially greater than the 480 to 1360 peak capacity range determined for IMS-IMS without 18C6 shift reagents.[22]

Analysis of Human Plasma Peptides with 18C6 Shift Reagent. With the added advantages in peak capacity and signal redundancy, it is interesting to apply the IMS-IMS technique to a system of extraordinary complexity. Our aim was to examine whether the IMS-IMS technique combined with 18C6 shift reagents could simplify a complex system to the point where distinct components could be isolated and identified by the single stage of mass spectrometry.

Figure 5 shows typical results for the analysis of a human plasma digest using IMS-IMS-MS with shift reagents. The proteome of human plasma is remarkable. It is believed that at any given time, on the order of 10^5 proteins may be present. Thus, we anticipate that more than a million peptide signals may exist. The largest signals should be associated with peptides from ∼40 abundant proteins that are known as the classical plasma proteins.[45] We (and others) have characterized plasma proteins from their tryptic peptides using a range of liquid chromatography and MS techniques.[42,46−48] Our findings (from a multi-dimensional separation involving strong-cation exchange and reversed phase liquid chromatography, coupled with IMS-MS detection) provided high-confidence identification of 2928 proteins (and many more signatures for species at lower confidence levels).[42] In direct IMS-MS analysis of tryptic peptides and peptide−18C6 mixtures (with no chromatography), spectra such as those shown in Figure 5 may contain $\sim 10^4-10^5$ features (and many distinct peaks).[42] A comparison of the IMS-MS results with MS-only (top panels of Figure 5) shows that many peptide−18C6 peaks that are buried under the baseline signal in the MS-only spectrum are apparent when the IMS separation is employed.

When ions are allowed to separate in the first IMS region and an activation gate is used to select narrow regions for further separation, the spectra are dramatically simplified. An example of this is also shown in Figure 5, for mobility-selection of a narrow distribution of ions having a total drift time of ∼32 ms (second panel). The mass spectrum that accompanies this selection indicates that many abundant peaks are present in this narrow drift time. Upon activation of these ions (using 165 V), the complexes dissociate. The resulting IMS-MS plot shows the

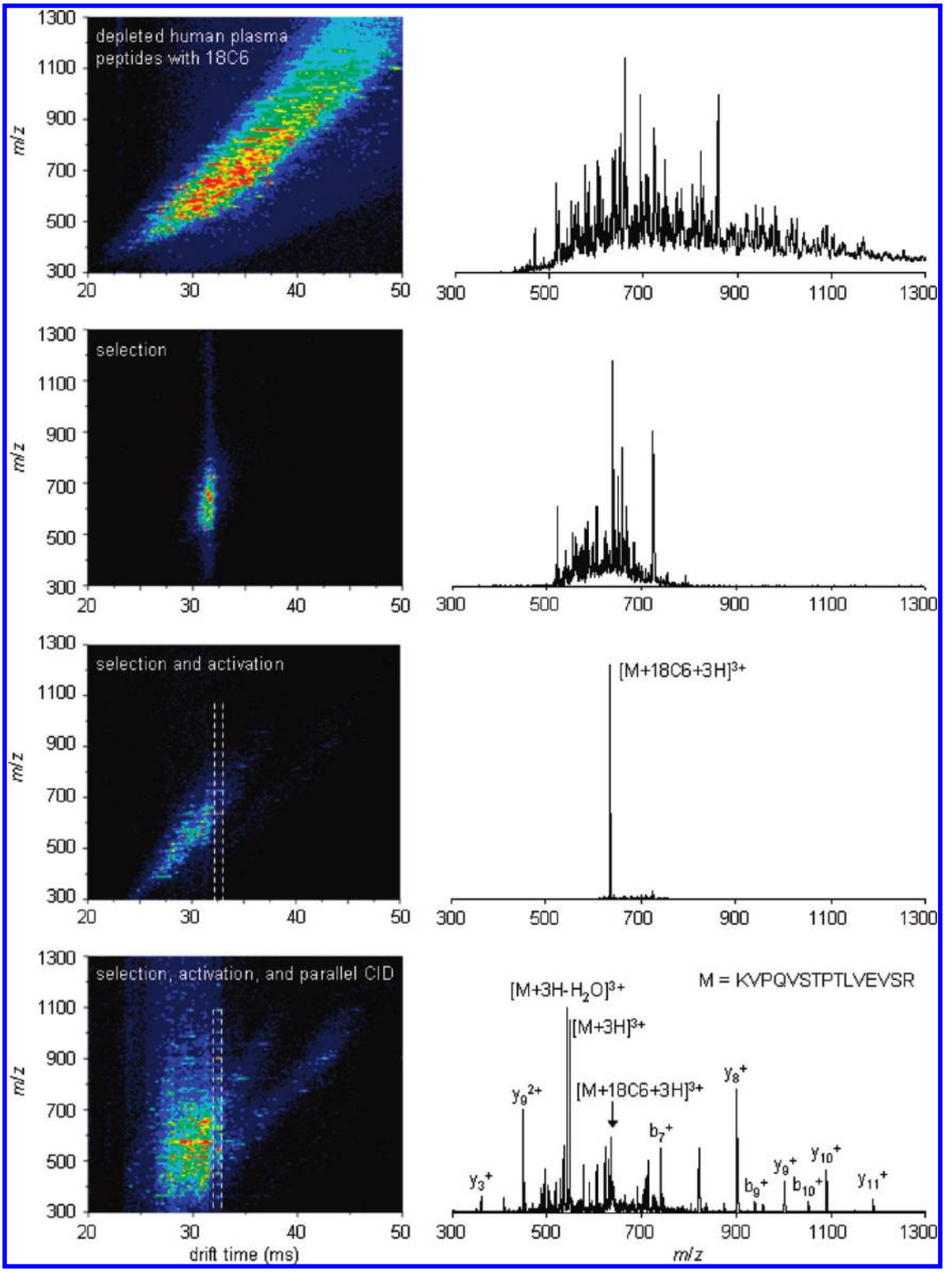

Figure 5. The top panel features an IMS-MS nested plot of human plasma peptides electrosprayed from a solution containing 18C6 with the total mass spectrum to the right. Mobility-selected complex ions (second panel) are activated with 165 V to dissociate the complex ions into bare peptide ions, which resolve further in mobility (third panel). Integration of the data between the dashed lines shows an isolated precursor in the drift dimension (third panel, right). Parallel dissociation at the end of the drift tube renders mobility-labeled fragments (fourth panel). Integration between the dashed lines now provides fragmentation spectrum that matches $[\mathrm{KVPQVSTPTLVEVSR} + 3\mathrm{H}]^{3+}$ (fourth panel, right). The ion score for this match was 43, well above the conservative statistical relevance threshold of 30.

advantage of the complexation approach. Large shifts in the m/z values and mobilities are observed. The smaller complexes and naked peptides lead to signals that are dispersed from ~24 to 32 ms. Such a large shift makes it possible to find regions that are

dx.doi.org/10.1021/ac200892r |*Anal. Chem.* 2011, 83, 5377–5385

dominated by a single peak (or a few peaks). A selection of a narrow region at 32 ms allows us to integrate a mass spectrum that is dominated by a peak at m/z = 635.3. Although other IMS times show similar simplification, we focus on this peak for assignment.

Our IMS-IMS-MS instrument is equipped with an activation region in the middle of the drift tube as well as one at the exit (as described previously).[16] When a set of mobility-separated ions is dissociated at the exit of the drift tube, we can align fragment peaks with their antecedent precursors (because the fragments and precursors are coincident in drift time). We refer to this as parallel dissociation.[49]

The final spectra shown in Figure 5 (bottom) correspond to parallel dissociation of precursors at the exit of the drift tube. These ions originated from the ESI source as peptide/18C6 complexes and were separated in an initial IMS region. A subset of these complexes was selected after the first IMS region, activated to dissociate the complexes, and then allowed to separate again prior to dissociation. In the present case we show dissociation of the precursor ion (that after these steps of separation is relatively isolated) at m/z = 635.3. The fragmentation spectrum for the isolated m/z = 635.3 ion can be obtained by integrating the signal at 32 ms. Upon activation, we find a large peak at m/z = 547.3, 88.0 Th less than the precursor state. This 88.0 Th difference is a signature of the loss of 18C6 from a triply charged peptide. An inspection of the isotopic spacing of the m/z = 547.3 peak confirms that this peak corresponds to a triply charged ion. The overwhelming majority of the remaining peaks correspond to singly charged species; there are no additional 88 Th differences, which if observed, would suggest that the m/z = 547.3 peak includes additional 18C6 molecules.

Thus, we begin interpreting this fragmentation pattern by assuming that the peak at m/z = 547.3 corresponds to a triply charged peptide ion precursor. Using this value and a list of peaks present in the spectrum as input for a database search, we find that our spectrum is likely due to the $[KVPQVSTPTLVEVSR + 3H]^{3+}$ peptide. This peptide is often detected in our plasma studies, as it arises from digestion of the most abundant protein in plasma, albumin. That we have identified this peptide directly with a single MS analysis suggests that the present approach has substantial utility. Other regions of the spectra show additional peptides from albumin as well as other proteins.[1] At this point in the analysis we have not characterized the range of protein abundances that can be detected directly with this approach. However, such an analysis requires only a few minutes to record and the early results appear promising.

Finally, it is interesting to note that peptide−18C6 complexes can be used directly for fragmentation studies to identify peptide sequences. Moreover, these methods may have merit in helping to define the charge states of precursor ions, when only low-resolution MS data are available.[50] As reported in previous CID studies on peptide−crown complexes,[26] 18C6 sequesters the charge on a protonation site and inhibits dissociation pathways involving a mobile proton.[51] The result of this is that the 18C6 adduct must dissociate before the proton can become mobile and induce substantial peptide bond breakage. Because 18C6 must be eliminated prior to peptide dissociation, fragmentation of a peptide−crown complex is probably less efficient compared to the corresponding naked peptide ion under identical conditions. Nonetheless, it appears that partially dissociated complexes can serve as precursor ions for fragmentation, should any of the naked peptide be recovered at low abundance or fail to isolate sufficiently in mobility.

SUMMARY AND CONCLUSIONS

We have examined IMS-IMS-MS analyses of tryptic peptides bound to 18C6 as a shift reagent. In this approach, electrosprayed peptide−crown complexes resolve in the first IMS dimension. A narrow distribution of complexes is mobility-selected and subsequently dissociated to yield a new distribution (including smaller complexes, naked peptides, charge transfer products, and fragments) which disperse in a second mobility separation. Analysis of a tryptic digest of cytochrome *c* using this approach shows increased IMS-IMS peak capacity (up to ∼2400) and detects two additional peptides compared to IMS-IMS alone. The peptides identified exclusively from the peptide−crown mixture correspond to sequences with missed cleavages and are presumably at lower abundance than the tryptic peptides.

An example of an analysis aimed at identifying a peptide from a complex mixture of peptides generated by digestion of human plasma was described. In this approach it was shown that this combination of techniques was sufficient to isolate an individual peptide from a direct-infusion electrospray ion source; and dissociation of the isolated peptide matched a peptide associated with an abundant protein in plasma.

While the ability to dissociate species increases the total IMS-IMS peak capacity (compared with only structural changes), the addition of 18C6 introduces a substantial increase in the complexity of the samples to be analyzed. This occurs because of the range of peptide−18C6 stochiometries and charge states, leading to multiple peaks for each peptide. On average, we estimate spectra to be a factor of ∼3.5 times more complex than those for peptides in the absence of 18C6. We note that only a few favorable cases (such as those highlighted here) may be needed to appreciably increase the information content of an analysis.

AUTHOR INFORMATION

Corresponding Author
*E-mail: clemmer@indiana.edu.

ACKNOWLEDGMENT

We acknowledge Amy Hilderbrand, Stormy Koeniger, and Samuel Merenbloom for helpful discussions during early stages of this project. This research was supported in part by the Indiana METACyt Initiative of Indiana University and a grant from the National Institutes of Health (Grant 1RC1GM090797-01).

REFERENCES

(1) For a recent review, see Bohrer, B. C.; Merenbloom, S. I.; Koeniger, S. L.; Hilderbrand, A. E.; Clemmer, D. E. *Annu. Rev. Anal. Chem.* **2008**, *1*, 293–327.

(2) Dwivedi, P.; Schultz, A. J.; Hill, H. H. *Int. J. Mass Spectrom.* **2010**, *298*, 78–90.

(3) Trimpin, S.; Tan, B.; Bohrer, B. C.; O'Dell, D. K.; Merenbloom, S. I.; Pazos, M. X.; Clemmer, D. E.; Walker, M. J. *Int. J. Mass Spectrom.* **2009**, *287*, 58–69.

(4) McLean, J. A. *J. Am. Soc. Mass Spectrom.* **2009**, *20*, 1775–1781.

(5) Fernandez-Lima, F. A.; Becker, C.; McKenna, A. M.; Rodgers, R. P.; Marshall, A. G.; Russell, D. H. *Anal. Chem.* **2009**, *81*, 9941–9947.

(6) Isailovic, D.; Kurulugama, R. T.; Plasencia, M. D.; Stokes, S. T.; Kyselova, Z.; Goldman, R.; Mechref, Y.; Novotny, M. V.; Clemmer, D. E. *J. Proteome Res.* **2008**, *7*, 1109–1117.

(7) Trimpin, S.; Clemmer, D. E. *Anal. Chem.* **2008**, *80*, 9073–9083.

(8) Plasencia, M. D.; Isailovic, D.; Merenbloom, S. I.; Mechref, Y.; Clemmer, D. E. *J. Am. Soc. Mass Spectrom.* **2008**, *19*, 1706–1715.

(9) McLean, J. A.; Ruotolo, B. T.; Gillig, K. J.; Russell, D. H. *Int. J. Mass Spectrom.* **2005**, *240*, 301–315.
(10) Tang, K. Q.; Li, F. M.; Shvartsburg, A. A.; Strittmatter, E. F.; Smith, R. D. *Anal. Chem.* **2005**, *77*, 6381–6388.
(11) Taraszka, J. A.; Gao, X.; Valentine, S. J.; Sowell, R. A.; Koeniger, S. L.; Miller, D. F.; Kaufmann, T. C.; Clemmer, D. E. *J. Proteome Res.* **2005**, *4*, 1238–1247.
(12) Gillig, K. L.; Ruotolo, B.; Stone, E. G.; Russell, D. H.; Fuhrer, K.; Gonin, M.; Schultz, A. J. *Anal. Chem.* **2000**, *72*, 3965–3971.
(13) Hoaglund-Hyzer, C. S.; Clemmer, D. E. *Anal. Chem.* **2001**, *73*, 177–184.
(14) Wu, C.; Siems, W. F.; Klasmeier, J.; Hill, H. H. *Anal. Chem.* **2000**, *72*, 391–395.
(15) Valentine, S. J.; Counterman, A. E.; Hoaglund, C. S.; Reilly, J. P.; Clemmer, D. E. *J. Am. Soc. Mass Spectrom.* **1998**, *9*, 1213–1216.
(16) Koeniger, S. L.; Merenbloom, S. I.; Valentine, S. J.; Jarrold, M. F.; Udseth, H. R.; Smith, R. D.; Clemmer, D. E. *Anal. Chem.* **2006**, *78*, 4161–4174.
(17) Merenbloom, S. I.; Koeniger, S. L.; Valentine, S. J.; Plasencia, M. D.; Clemmer, D. E. *Anal. Chem.* **2006**, *78*, 2802–2809.
(18) Valentine, S. J.; Kurulugama, R. T.; Bohrer, B. C.; Merenbloom, S. I.; Sowell, R. A.; Mechref, Y.; Clemmer, D. E. *Int. J. Mass Spectrom.* **2009**, *283*, 149–160.
(19) Koeniger, S. L.; Clemmer, D. E. *J. Am. Soc. Mass Spectrom.* **2007**, *18*, 322–331.
(20) Koeniger, S. L.; Merenbloom, S. I.; Clemmer, D. E. *J. Phys. Chem. B* **2006**, *110*, 7017.
(21) Koeniger, S. L.; Merenbloom, S. I.; Sevugarajan, S.; Clemmer, D. E. *J. Am. Chem. Soc.* **2006**, *126*, 11713–11719.
(22) Merenbloom, S. I.; Bohrer, B. C.; Koeniger, S. L.; Clemmer, D. E. *Anal. Chem.* **2007**, *79*, 515–522.
(23) Hilderbrand, A. E.; Myung, S.; Clemmer, D. E. *Anal. Chem.* **2006**, *78*, 6792–6800.
(24) Howdle, M. D.; Eckers, C.; Laures, A. M. F.; Creaser, C. S. *J. Am. Soc. Mass Spectrom.* **2009**, *20*, 1–9.
(25) Aebersold, R.; Mann, M. *Nature* **2003**, *422*, 198–207.
(26) Lee, S.-W.; Lee, H.-N.; Kim, H. S.; Beauchamp, J. L. *J. Am. Chem. Soc.* **1998**, *120*, 5800–5805.
(27) Williamson, B. L.; Creaser, C. S. *Int. J. Mass Spectrom.* **1999**, *188*, 53–61.
(28) Julian, R. R.; Beauchamp, J. L. *Int. J. Mass Spectrom.* **2001**, *210/211*, 613–623.
(29) Dearden, D. V.; Liang, Y.; Nicoll, J. B.; Kellersberger, K. A. *J. Mass Spectrom.* **2000**, *36*, 989–997.
(30) Weimann, D. P.; Winkler, H. D. F.; Falenski, J. A.; Koksch, B.; Schalley, C. A. *Nat. Chem.* **2009**, *1*, 573–577.
(31) St. Louis, R. H.; Hill, H. H. *Crit. Rev. Anal. Chem.* **1990**, *21*, 321–355.
(32) Meslah, M. F.; Hunter, J. M.; Shvartsburg, A. A.; Schatz, G. C.; Jarrold, M. F. *J. Phys. Chem.* **1996**, *100*, 16082–16086.
(33) Wyttenbach, T.; von Helden, G.; Batka, J. J.; Carlat, D.; Bowers, M. T. *J. Am. Soc. Mass Spectrom.* **1997**, *8*, 275–282.
(34) Clemmer, D. E.; Jarrold, M. F. *J. Mass Spectrom.* **1997**, *32*, 577–592.
(35) Hoaglund-Hyzer, C. S.; Counterman, A. E.; Clemmer, D. E. *Chem. Rev.* **1999**, *99*, 3037–3079.
(36) Hoaglund, C. S.; Valentine, S. J.; Sporleder, C. R.; Reilly, J. P.; Clemmer, D. E. *Anal. Chem.* **1998**, *70*, 2236–2242.
(37) Srebalus Barnes, C. A.; Clemmer, D. E. *Anal. Chem.* **2001**, *73*, 424–433.
(38) Mason, E. A.; McDaniel, E. W. *Transport Properties of Ions in Gases*; Wiley: New York, 1988.
(39) Perkins, D. N.; Pappin, D. J. C.; Creasy, D. M.; Cottrell, J. S. *Electrophoresis* **1999**, *20*, 3551–3567.
(40) Valentine, S. J.; Counterman, A. E.; Clemmer, D. E. *J. Am. Soc. Mass Spectrom.* **1999**, *10*, 1188–1211.
(41) Valentine, S. J.; Counterman, A. E.; Hoaglund, C. S.; Reilly, J. P.; Clemmer, D. E. *J. Am. Soc. Mass Spectrom.* **1998**, *9*, 1213–1216.
(42) Liu, X.; Valentine, S. J.; Plasencia, M. D.; Trimpin, S.; Naylor, S.; Clemmer, D. E. *J. Am. Soc. Mass Spectrom.* **2007**, *18*, 1249–1264.
(43) Pierson, N. A.; Valentine, S. J.; Clemmer, D. E. *J. Phys. Chem. B* **2010**, *114*, 7777–7783.
(44) Giddings, J. C. *Unified Separation Science*; Wiley: New York, 1991.
(45) Anderson, N. L.; Anderson, N. G. *Mol. Cell. Proteomics* **2002**, *1*, 845–867.
(46) Adkins, J. N.; Varnum, S. M.; Auberry, K. J.; Moore, R. J.; Angell, N. H.; Smith, R. D.; Springer, D. L.; Pounds, J. G. *Mol. Cell. Proteomics* **2002**, *1*, 947–955.
(47) Tirumalai, R. S.; Chan, K. C.; Prieto, D. A.; Issaq, H. J.; Conrads, T. P.; Veenstra, T. D. *Mol. Cell. Proteomics* **2003**, *2*, 1096–1103.
(48) Pieper, R.; Gatlin, C. L.; Makusky, A. J.; Russo, P. S.; Schatz, C. R.; Miller, S. S.; Su, Q.; McGrath, A. M.; Estock, M. A.; Parmar, P. P.; Zhao, M.; Huang, S. T.; Zhou, J.; Wang, F.; Esquer-Blasco, R.; Anderson, N. L.; Taylor, J.; Steiner, S. *Proteomics* **2003**, *3*, 1345–1364.
(49) Hoaglund-Hyzer, C. S.; Li, J.; Clemmer, D. E. *Anal. Chem.* **2000**, *72*, 2737–2740.
(50) Cunniff, J. B.; Vouros, P. *Rapid Commun. Mass Spectrom.* **1994**, *8*, 715–719.
(51) Dongré, A. R.; Jones, J. L.; Somogyi, Á.; Wysocki, V. H. *J. Am. Chem. Soc.* **1996**, *118*, 8365–8374.